First-passage distributions in a collective model of anomalous diffusion with tunable exponent

Assaf Amitai,[1] Yacov Kantor,[1] and Mehran Kardar[2]
[1]*Raymond and Beverly Sackler School for Physics and Astronomy, Tel Aviv University, Tel Aviv 69978, Israel*
[2]*Department of Physics, Massachusetts Institute of Technology, Cambridge, Massachusetts 02139, USA*
(Received 18 September 2009; published 6 January 2010)

We consider a model system in which anomalous diffusion is generated by superposition of underlying linear modes with a broad range of relaxation times. In the language of Gaussian polymers, our model corresponds to Rouse (Fourier) modes whose friction coefficients scale as wave number to the power $2-z$. A single (tagged) monomer then executes subdiffusion over a broad range of time scales, and its mean square displacement increases as t^{α} with $\alpha=1/z$. To demonstrate nontrivial aspects of the model, we numerically study the absorption of the tagged particle in one dimension near an absorbing boundary or in the interval between two such boundaries. We obtain absorption probability densities as a function of time, as well as the position-dependent distribution for unabsorbed particles, at several values of α. Each of these properties has features characterized by exponents that depend on α. Characteristic distributions found for different values of α have similar qualitative features, but are not simply related quantitatively. Comparison of the motion of translocation coordinate of a polymer moving through a pore in a membrane with the diffusing tagged monomer with identical α also reveals quantitative differences.

DOI: 10.1103/PhysRevE.81.011107 PACS number(s): 05.40.−a, 02.50.Ey, 87.15.A−

I. INTRODUCTION

In many physical processes one encounters a stochastic variable whose mean squared fluctuations increase with time t as t^{α} with $\alpha \neq 1$. These processes are sometimes referred to as anomalous diffusion [1], and specifically *subdiffusion* for $\alpha<1$. Such behavior is usually caused by the collective dynamics of numerous degrees of freedom, or modes with a broad distribution of characteristic times. The exact relations between the underlying modes and the observed coordinate are usually unknown, and first-principle derivation of the equations governing the anomalous diffuser are rare. As a result, a variety of such processes are typically grouped into broad classes in accordance to their general characteristics [2]. While the exponent α is an important and convenient indicator of anomalous dynamics, it contains little information on the hidden underlying driving forces.

A different set of properties of a diffuser can be revealed by observing its *first passage* to a target, or its absorption at a trap [3–5]. For instance, it has been established [6] that the probability density function (PDF) $Q(t)$ to be absorbed for one-dimensional (1D) subdiffusion between two absorbing walls has a power-law tail, if the process is described by a fractional diffusion equation [2]. This slow decay of $Q(t)$ for a subdiffuser following such dynamics leads to a diverging mean absorption time. On the other hand, Kantor and Kardar [7] demonstrated that a monomer in a Gaussian polymer that is characterized by $\alpha=1/2$ has a finite absorption time when it diffuses between two absorbing boundaries. The presence of absorbing boundaries introduces additional characteristics, such as the long-time behavior of the survival probability $S(t)$ in the presence of a single absorbing wall, or the behavior of the PDF of particle position near the trap. In specific cases with a well-defined α (see, e.g., Refs [8,9]) some aspects of absorption characteristics have been determined. However, in the absence of rigorous scaling relations one cannot establish whether the exponent α determines all other characteristics. Recently, Zoia *et al.* [10] used some general scaling arguments to propose such a relation, furthering the need to probe such properties with tunable exponent α.

While it is generally recognized that underlying (hidden) processes are responsible for anomalous dynamics, many theoretical approaches simplify the problem to effective equations for the observed variable, hoping to capture the multitude of underlying interactions. There is no *a priori* reason for such an approach to succeed, and it is therefore useful to consider alternative models where the underlying processes are well characterized. In this work we consider a model in which subdiffusion is generated as a result of superposition of underlying modes with a broad range of time scales. For solvability and ease of simulation we limit ourselves to linear (but stochastic) dynamics for the modes. Our model is closely related to the dynamics of a Gaussian polymer, or to fluctuations of a Gaussian interface. In the polymer language, which we adapt for most of the presentation, the anomalous behavior of a single (tagged) monomer [11] is easily understood in terms of the superposition of underlying Rouse modes. The resulting exponent α depends on whether the polymer dynamics is diffusive (Rouse) or influenced by hydrodynamic interactions (Zimm). The difference between the two cases can be cast as due to a wavelength dependent friction coefficients.

In Sec. II B we take this analogy a step further, and show that any value of α can be generated by appropriate scaling of the friction coefficients with wavelength. While we adapt notions from polymer physics in developing our model, the approach we take is not intended to address any particular polymer problem. Rather, we rely on this well-defined mathematical model to explore issues pertinent to anomalous diffusion (specifically absorption), and to compare and contrast with other mathematical models introduced in this context. Our approach is closely related to the model proposed by Krug *et al.* [12] where the value of α is controlled by modifying the forces between particles. We use our generalization to study anomalous diffusion in the presence of one and two

absorbing boundaries in Secs. III A and III B In particular, we explore the long-time tails of the absorption probability $Q(t)$, as well as the asymptotic stable shapes of the PDFs of the surviving walkers. Qualitatively, various quantities have similar features for a variety of α. However, we find that α does not enter the results in a trivial way, and the stable function for one α cannot be obtained from another by simple transformation. Moreover, the comparison of results for our walker with exponent α coinciding with that of a polymer translocating though a membrane pore (Sec. IV A) demonstrates quantitative differences between the two cases. Some possible extensions of this work are discussed in Sec. IV B.

II. MODEL

A. Rouse modes of polymers and anomalous dynamics of a monomer

Polymers [13] provide a relatively simple physical system in which the collective motion of monomers leads to behavior spanning a broad range of time scales [14]. Ignoring the interactions between non-covalently-bonded monomers, the dynamics of a polymer can be reduced to independent Rouse (Fourier) modes [15]. For a polymer consisting of N monomers, each such mode U_p $(p=0,\ldots,N-1)$ has a distinct relaxation time τ_p. The Gaussian (or ideal) polymer is a particularly simplified model composed of beads (monomers) connected by harmonic (Gaussian) springs. Each polymer configuration is now described by the set of monomer positions R_n $(n=1,2,\ldots,N)$, and has energy (again neglecting further neighbor interactions)

$$H=\frac{\kappa}{2}\sum_{n=1}^{N}(R_n-R_{n-1})^2. \tag{1}$$

Here the spring constant is $\kappa=k_BT/b^2$, where k_B is the Boltzmann constant, T is the temperature, and b is the root-mean-square distance between a pair of connected monomers.

From Eq. (1) we can construct a simple relaxational (Langevin) dynamics for the Gaussian polymer, whereby

$$\zeta\frac{dR_n}{dt}=-\kappa(2R_n-R_{n+1}-R_{n-1})+f_n, \tag{2}$$

for $1<n<N$. The deterministic force (first term on the right-hand side) is different for R_1 and R_N, since the end monomers are attached only to a single neighbor. Here, ζ is the friction coefficient of the monomer, while the noise $f_n(t)$ has a zero mean and correlations of $\langle f_n(t)f_m(t')\rangle=2\zeta k_BT\delta_{n,m}\delta(t-t')$, to ensure proper thermal equilibrium at temperature T. In one dimension the positions $\{R_n\}$ are scalars, while the generalization to vectorial coordinates in higher dimensions is trivial, as in this model the coordinates in different spatial dimensions are independent.

Rouse modes are now obtained by Fourier transformation as [14]

$$U_p=\frac{1}{N}\sum_{n=1}^{N}R_n\cos\left[\frac{(2n-1)p\pi}{2N}\right], \tag{3}$$

where $p=0,1,\ldots,N-1$ is the mode number and U_p is the mode amplitude. (The choice of cosines automatically takes care of the modified equations for R_1 and R_N.) The Rouse coordinates are decoupled and evolve according to [14]

$$\zeta_p\frac{dU_p}{dt}=-\kappa_pU_p+W_p, \tag{4}$$

where $\kappa_p=8N\kappa\sin^2(\frac{p\pi}{2N})$, and $\zeta_p=2N\zeta$ for $p\geq 1$, and $\zeta_0=N\zeta$. The noise W_p has again zero mean and correlations of

$$\langle W_p(t)W_{p'}(t')\rangle=2k_BT\zeta_p\delta_{p,p'}\delta(t-t'). \tag{5}$$

Note that the $N-1$ *internal modes* for $p\neq 0$ behave as particles tethered by a harmonic spring, while the center of mass (CM), corresponding to $p=0$, freely diffuses.

The linear Eqs. (4) are readily solved starting from any initial condition, and the probabilities for $\{U_p\}$ are Gaussians, with a time-dependent mean set by initial conditions, and a variance

$$\sigma_p^2=\frac{k_BT}{\kappa_p}(1-e^{-2t/\tau_p}),\quad \text{for}\quad p\geq 1,$$

$$\sigma_0^2=2D_{\mathrm{CM}}t. \tag{6}$$

The equilibration (relaxation) times of the internal modes are $\tau_p=\zeta_p/\kappa_p$, while the diffusion constant is $D_{\mathrm{CM}}=k_BT/N\zeta$. There is clearly a hierarchy of relaxation times: the shortest time scale $\tau_{N-1}\approx\zeta/(4\kappa)$ is half of the time $\tau_s=\zeta/(2\kappa)$ during which a *free* monomer diffuses a mean squared distance between the adjacent monomers, $b^2=k_BT/\kappa$. For the CM, we can define a characteristic time $\tau_0\equiv b^2N/D_{\mathrm{CM}}=N^2\zeta/\kappa$ associated with diffusing over the size of the polymer. This is of the same order as the longest internal relaxation time τ_1; for long polymers $\tau_0/\tau_1\approx\pi^2$.

By inverting Eq. (3) one can also follow the position of a specific ("tagged") monomer, as

$$R_n=U_0+2\sum_{p=1}^{N-1}U_p\cos\left[\frac{(2n-1)p\pi}{2N}\right]. \tag{7}$$

This equation becomes particularly simple for the central monomer $c=(N+1)/2$ (assuming odd N), as

$$R_c=U_0+2\sum_{k=1}^{(N-1)/2}(-1)^kU_{2k}. \tag{8}$$

Since each term in the above sum is (independently) Gaussian distributed, so is R_c, with variance

$$\mathrm{var}(R_c)=\sigma_0^2+4\sum_{k=1}^{(N-1)/2}\sigma_{2k}^2. \tag{9}$$

Utilizing Eq. (6), we can now distinguish between three regimes:

(1) For short times $t\ll\tau_s$, we can expand the exponential in Eq. (6) and obtain $\sigma_p^2\approx k_BTt/(N\zeta)$ independent of p. The

sum in Eq. (9) then leads to $\mathrm{var}(R_c) \approx 2D_s t$, with a monomer diffusion constant of $D_s = k_B T/\zeta$.

(2) For very long times $t \gg \tau_1$ all the internal modes saturate to a variance that is independent of t. In this regime the additional time dependence comes from the first term in Eq. (9) corresponding to the slow diffusion of the center of mass.

(3) The most interesting regime is for intermediate times, with $\tau_s \ll t \ll \tau_0$, where only the terms for which $2t/\tau_{2k} > 1$ will contribute significantly to Eq. (9). Focusing on the corresponding modes, we obtain

$$\mathrm{var}(R_c) \approx 4 \int_{k=k_{\min}}^{N/2} \frac{k_B T}{\kappa_{2k}} dk, \tag{10}$$

where $k_{\min}$ is determined from the relation $\tau_{2k_{\min}} = 2t$. Using the usual expression for τ_p of the Gaussian polymer one can immediately see that $\mathrm{var}(R_c) \sim t^{1/2}$. This interval clearly exhibits anomalous diffusion due to the collective behavior of the modes; its size can be made arbitrarily long by letting $N \to \infty$.

B. Generalized modes with variable exponent

In Ref. [7] the tagged monomer was used as a prototype of subdiffusion. Of course, as described so far the anomalous dynamics of the tagged monomer is characterized by the exponent $\alpha = 1/2$. It is possible to modify Eq. (4) in different ways so as to produce dynamics for any value of α. We shall do so by considering power-law dependences of the friction coefficients ζ_p on the mode-index p, as motivated by the following two physical models:

(1) Zimm analyzed the motion of a polymer in the presence of hydrodynamic flows, which result in interactions that decay (in three dimensions) as an inverse distance between monomers. These interactions do not change the probability distribution in configuration space (which is still governed by the equilibrium Boltzmann weight), but do modify the relaxation times. Zimm showed [16] that the resulting dynamics can be *approximately* described by Eq. (4), but with $\zeta_p \propto p^{1/2}$. We can now work through the same steps as in the previous section, and find anomalous diffusion for the tagged monomer, but with exponent $\alpha = 2/3$.

(2) Equation (1) can also be regarded as the energy of a fluctuating stretched line, with $\{R_n\}$ indicating the heights above a baseline [12,17]. If the line separates two phases of fixed volume, the sum $\Sigma_n R_n$ must remain unchanged under the dynamics. Such *conserved dynamics* are mimicked by Eq. (4), but with $\zeta_p \propto p^{-2}$ [17]. As long as the noise correlations satisfy Eq. (5) the equilibrium distribution remains unchanged, but the dynamics is slowed down, such that the fluctuations of a given coordinate now evolve with exponent $\alpha = 1/4$.

Motivated by the above examples, we consider dynamics according to Eqs. (4) and (5) with generalized ζ_p given by

$$\zeta_p = 2CN\zeta \left(\frac{p}{N}\right)^{2-z}, \quad \text{for } p \geq 1,$$

$$\zeta_0 = \zeta N^{z-1}. \tag{11}$$

The choice of exponent z leads to time scales

$$\tau_p = \frac{C\zeta (p/N)^{2-z}}{4\kappa \sin^2(p\pi/2N)} \approx C\frac{\zeta}{\kappa \pi^2}\left(\frac{N}{p}\right)^z, \tag{12}$$

where the last approximation is valid for $p \ll N$. The longest internal mode scales with the number of degrees of freedom as N^z. This is the conventional notation for the dynamic exponent of a fluctuating line, or a free-field theory, but somewhat different from that used to denote the relaxation of polymers. The Rouse, Zimm, and conserved models correspond to $z = 2$, 3/2, and 4, respectively. The dimensionless constant $C = 2\zeta_1/\zeta_0$ is somewhat arbitrary. It defines the ratio between the time characterizing the diffusion of the CM and the relaxation time of the slowest internal mode. We chose it in a way that for very short times the motion of R_c has a diffusion constant of $D_s = k_B T/\zeta$ irrespective of z. For large N this leads to $C = 1/(z-1)$. We would like to stress that Zimm dynamics, as well as other physical systems producing anomalous diffusion, are only *approximately* described by Eq. (4) with length-scale dependent friction constants. However, we employ Eqs. (4) and (11) as the (exact) definition of our mathematical model for anomalous diffusion with tunable exponents.

Focusing on the coordinate R_c (the tagged monomer), we observe that it executes normal diffusion with diffusion coefficient D_s for times $t \ll \tau_s = \zeta/2\kappa$. For very long times $t \gg \tau_0 = (\zeta/\kappa)N^z$ it again performs regular diffusion but with a much smaller center of mass diffusion coefficient of D_s/N^{z-1}. At intermediate times $\tau_s < t < \tau_0$, fluctuations of R_c are influenced by the p-dependent relaxation times in Eq. (12), and evolve anomalously as $\mathrm{var}(R_c) \propto t^\alpha$. The exponent α can be obtained simply by noting [11] that at times of order τ_0, $\mathrm{var}(R_c)$ should be similar to typical equilibrium (squared) size of the polymer, which grows as $Nk_B T/\kappa$. Equating these two quantities immediately yields

$$\mathrm{var}(R_c) = Kb^2 \left(\frac{D_s t}{b^2}\right)^\alpha, \tag{13}$$

where K is a dimensionless prefactor, and

$$\alpha = \frac{1}{z}. \tag{14}$$

This result can also be directly obtained from Eqs. (10) and (12).

In Ref. [12] an alternative strategy is employed for obtaining a tunable exponent, namely by scaling the "spring constant" in Eq. (4) as $\kappa_p^{2/z}$, while leaving the friction coefficients ζ_p unchanged. Without a corresponding scaling of the noise amplitudes W_p, the steady state probability is now also modified. The simulations of Ref. [12] are actually obtained by evolving the Langevin equations in real space (as opposed to Fourier mode evolutions performed in our current work). This necessitates generalizing the interactions in Eq. (2) to further neighbors, and/or generating correlated noise in real space. Nevertheless, for $z = 2$ the two approaches should be identical—corresponding to Gaussian polymers—and direct comparison should be possible.

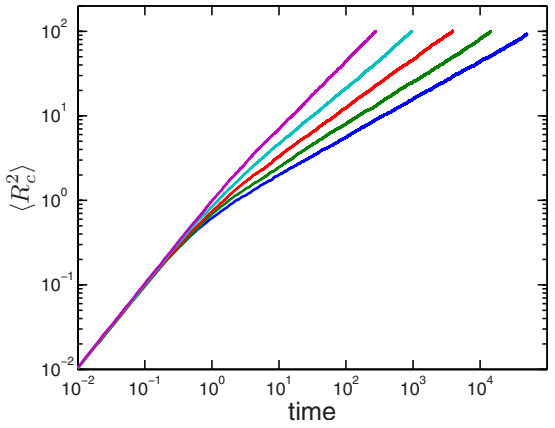

FIG. 1. (Color online) Mean squared position of the central monomer (in units of b^2) as a function of time (in units of τ_s) for a polymer of length $N=257$. The curves correspond (left to right) to $z=1.25$, 1.5, 1.75, 2, and 2.25. Each curve is an average over 10 000 realizations.

C. Numerical implementation

To verify the dependence of the anomalous exponent on z, we simulated the dynamics of a chain of $N=257$ monomers by numerically solving the Langevin equation for each of the modes. At the beginning of each simulation we equilibrated the polymer by randomizing the initial mode amplitudes, and positioned the central monomer ($c=129$) at the origin. The position R_c of the central monomer was evolved by numerically integrating the Langevin Eqs. (4) with the smart Monte Carlo method [18], followed by transforming the mode amplitudes U_p to the monomer position space, at each time step. Figure 1 illustrates the results for several values of z. The averages of R_c^2 were calculated over 10 000 independent simulations. For each value of z the times are at least an order of magnitude shorter than the slowest relaxation mode of the polymer for that z. For $t<\tau_s$ the curves coincide: in that region the particles perform normal diffusion with diffusion constant D_s which is independent of z. For $t>\tau_s$ we can clearly observe a pure power-law growth with exponent $\alpha=1/z$ confirming Eq. (14). Using our model it is possible to get very slow dynamics $\alpha\to 0$ by taking $z\gg 1$, or to reproduce $\alpha=1$ by setting $z=1$.

We also verified that the probability density of the distribution of R_c is a Gaussian. The Langevin equation describing each U_p can be solved analytically, and consequently the parameters of the Gaussian distribution for R_c (its mean and variance) are known. Thus, the numerical results presented in Fig. 1 were anticipated, and primarily served to evaluate the accuracy of the numerical procedure. In the following sections we will use the same procedure for results that cannot be found analytically.

III. RESULTS

The behavior of a particle near absorbing boundaries may reveal aspects of the dynamics not apparent in the scaling of the mean square displacement. Indeed, consideration of absorption of a monomer in a simple Gaussian polymer [7] have provided novel insights into the differences between different forms of anomalous dynamics with $\alpha=1/2$. In our numerical studies, we implemented anomalous diffusion as described in Sec. II C, but with *only the tagged monomer interacting with the absorbing boundaries*. For the case of a single absorbing boundary, for each z, the starting position $x(0)$ of the tagged monomer was at a distance $8b$ away from the absorbing boundary, while for the case of two absorbing boundaries the monomer was placed between them at a distance $8b$ from either one. The numerical procedure imposes both lower and upper limits on the relevant times:

(1) If the tagged monomer is initially located at a distance $x(0)$ from an absorbing boundary, a sufficiently long time is required for the probability density to be influenced by absorption. Since the typical squared distance traveled by anomalous diffusers is given by Eq. (13), the absorption probability becomes significant after a time (disregarding the dimensionless prefactor K)

$$T=(b^2/D_s)[x(0)/b]^{2/\alpha}=2\tau_s[x(0)/b]^{2/\alpha}. \tag{15}$$

In our simulations with $x(0)=8b$, and for $z=1.25$ (2.25) this leads to $T\approx 360\tau_s$ ($2.3\times 10^4\tau_s$). Alternatively, one can find directly from Eq. (9), that for $z=1.25$ (2.25) the quantity $\langle R_c^2\rangle$ reaches $64b^2$ at time $T'\approx 160\tau_s$ ($2.3\times 10^4\tau_s$). (Graphically, T' can be found simply from Fig. 1 as the time corresponding to $64b^2$.) The fact that T' is not strictly proportional to T, is related to the z dependence of K, since z enters Eqs. (11) through the constant C.

(2) Anomalous diffusion is expected for times significantly shorter than the longest relaxation time $\tau_0\approx\tau_s N^z$; for $z=1.25$ (2.25) and $N=257$, we estimate $\tau_0\approx 10^3\tau_s$ ($2.6\times 10^5\tau_s$). [Since $\tau_1\approx\tau_0/[(z-1)\pi^2]$ [see Eq. (12)], the corresponding values of the slowest internal modes are $400\tau_s$ ($2.1\times 10^4\tau_s$).] In the presence of a single absorbing boundary our simulation times for $z=1.25$ (2.25) were shorter than $1.6\times 10^3\tau_s$ ($1.6\times 10^4\tau_s$), while for the case of two absorbing boundaries they were shorter than $600\tau_s$ ($6.5\times 10^3\tau_s$). These numbers indicate that most of our simulations stayed within the anomalous diffusion regime. To verify this point we performed simulations for $N=65$, 129, and 257 for $z=2$ and observed the convergence of their absorption time distributions, which indicates that we are in the N-independent regime. In the following we report only the results for the central monomer $c=129$ of the chains with $N=257$.

A. Absorption time distribution

1. Single absorbing boundary

The problem of a particle performing normal diffusion in the presence of absorbing boundaries has been described in detail by Chandrasekhar [19]. It can be cast as a simple (linear) diffusion equation for the evolving probability density, with vanishing boundary conditions at the absorbing points. In the presence of one absorbing boundary in 1D, an elegant solution is found by the method of images [4,19], i.e., by subtracting from the Gaussian solution describing the probability density in the absence of absorption, a similar Gaussian centered at the "mirror image position" with respect to the absorbing boundary. At times shorter than $T=x^2(0)/D$,

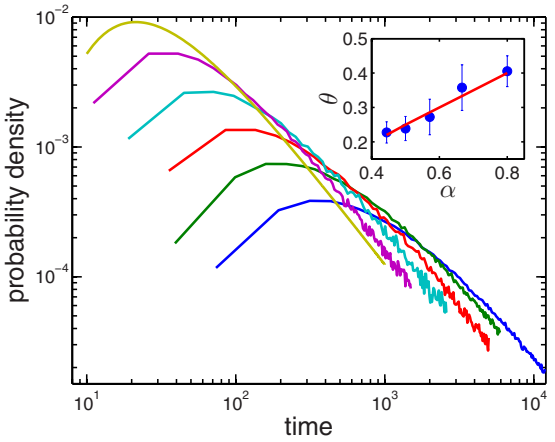

FIG. 2. (Color online) Logarithmic plot of absorption probability distribution as a function of time (in units of τ_s) of the central monomer of a $N=257$ polymer, in the presence of an absorbing boundary at a distance $8b$ from the initial position of the monomer. The leftmost curved depicts the result for normal diffusion of a single particle. The rest of the curves correspond (left-to-right) to $z=1.25$, 1.5, 1.75, 2, and 2.25. For each z value, 100 000 independent runs were performed. The inset depicts the value of θ obtained from the slopes of these graphs as a function of α. The continuous line depicts the relation between these exponents proposed in Ref. [20] (see text).

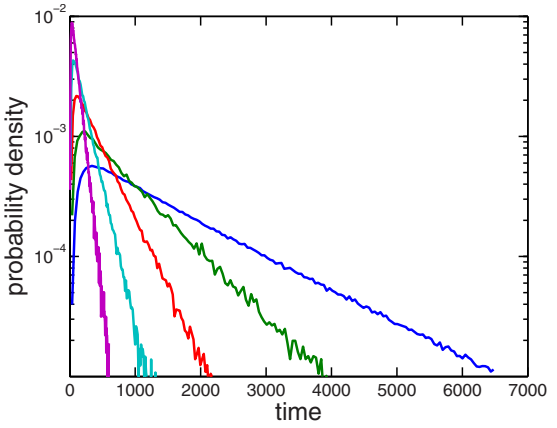

FIG. 3. (Color online) Semilogarithmic plot of the absorption probability density of a tagged monomer as a function of time (in units of τ_s) for the central monomer in a $N=257$ polymer, in the interval between two absorbing boundaries at a distance $16b$. The monomer starts at the midpoint between the boundaries. Each curve is the result of 100 000 independent simulations. The different curves correspond (left to right) to $z=1.25$, 1.5, 1.75, 2, and 2.25.

where D is the diffusion constant of the particle and $x(0)$ is its initial distance from the boundary, the particle does not feel the absorbing boundary. For $t \gg T$ the survival probability (obtained by integrating the solution over the allowed interval) scales as $S(t) \sim t^{-1/2}$, while the absorption PDF behaves as $Q(t) = -dS/dt \sim t^{-3/2}$. We note that the mean absorption time is infinite, since the particle can survive indefinitely by diffusing away from the absorbing boundary.

Figure 2 depicts on a logarithmic scale the PDFs of the absorption $Q(t)$ of the tagged monomer initially located at distance $x(0)=8b$ from a single absorbing boundary for different values of z. (For comparison, results for normal diffusion of a single particle are also shown.) Absorption is negligible at short times, but gradually increases to a maximum at a time significantly smaller than T defined by Eq. (15). As in the case of normal diffusion, it is generally accepted that the absorption PDF decays as a power law $Q(t) \sim t^{-1-\theta}$ at long times; $\theta=1/2$ for regular diffusers while any $\theta \leq 1$ leads to a diverging mean absorption time. We attempted to extract the exponent θ from the slopes of the curves in the logarithmic plot in Fig. 2 at large values of t. While 10^4 independent runs were performed to obtain each of the curves, only a small fraction of diffusers survived to times significantly longer than the position of the maximum. Nevertheless, for each z we have reasonably accurate results for 1.5 decades beyond the time of maximal $Q(t)$. Only the second half of this interval (on a logarithmic scale) is a straight line, and it was used to evaluate θ. There are thus significant statistical errors in the estimates for θ as depicted by the error bars in the inset of Fig. 2.

Studies of continuous time random walks using the fractional Fokker-Planck equation [20] obtain a simple relation $\theta=\alpha/2$ for $0<\alpha<2$. This relation is depicted by the continuous line in the inset. Although there is no sound theoretical foundation for applying this relation to the collective anomalous diffusion of our model, we note that there is some correspondence between the line and the measured exponents. In Ref. [12] an alternative relation $\theta=1-\alpha/2$ is proposed, based on considerations of fractional Brownian motion. Neither the values, nor the trend in this relation are consistent with the results in Fig. 2. We are puzzled by this discrepancy as Ref. [12] also provides numerical support for this relation, and the method used (although somewhat distinct in general) should essentially coincide with ours for the case of $z=2$ ($\alpha=1/2$). We are reluctant to make a definite statement regarding this exponent, as in addition to the statistical errors (error bars in the inset in Fig. 2) there are uncertainties due to possible systematic errors: the measurements of θ are performed for times one order of magnitude larger that of the maximum of $Q(t)$. These times do not significantly exceed T or T', and are possibly even shorter than the latter, especially for larger values of z. Getting rid of such possible systematic errors requires significantly larger N and more statistical samples, but is clearly needed to resolve this discrepancy.

2. Two absorbing boundaries

We also considered a tagged monomer confined in the interval between two absorbing boundaries separated by $16b$. Initially the particle is placed half-way between the two boundaries, i.e., at a distance $8b$ from each. Figure 3 illustrates on a semilogarithmic plot, the absorption probability $Q(t)$ for different values of z. The distributions have the same general shape as before, with absorption probability rising with time to a maximum. However, the fall off at long times appears to be exponential. The straight lines in the semilogarithmic plots clearly rule out the stretched exponential decay characterizing other forms of anomalous diffusion [21]. They also bear no resemblance to the power-law decay (with di-

verging mean absorption time) expected for subdiffusion described by the fractional Fokker-Plank equation [6]. The mean absorption time and the typical decay time (as determined from exponential decay) are practically indistinguishable for each z. They are, however, by more than an order of magnitude shorter than the typical time T defined by Eq. (15) or T'.

B. Long-time distribution of particle position

1. Single absorbing boundary

Let us now consider the dependence on the coordinate x of the PDF $p(x,t|x(0))$, starting at an initial position $x(0)$ from a single absorbing boundary at $x=0$. As noted before, for a regularly diffusing particle this PDF is obtained by the method of images as the difference between Gaussians centered at $\pm x(0)$, whose width grows as $\ell(t)=\sqrt{D_s t}$. Expanding this solution close to the boundary, we find $p[x,t|x(0)] \approx xx(0)/\ell(t)^3$, i.e., the PDF vanishes linearly with x in the vicinity of the boundary. It is tempting to generalize this result to anomalous diffusion, by simply replacing the scaling form of the width by $\ell(t)=b^{1-\alpha}(D_s t)^{\alpha/2}$, and again concluding a linear behavior with x albeit with a different dependence on t. However, the method of images relies on the absence of memory in the motion [19], which is not correct for our non-Markovian processes. Indeed in a previous study we observed that for the case of $\alpha=1/2$ the vanishing of the PDF near an absorbing boundary is faster than linear. (A similar problem occurs when a diffuser performs Lévy flights, since the absorbing boundary is no longer a turning point of the trajectory [9,22].) We shall assume that for $t \gg T$ [Eq. (15)] the behavior near the boundary can be described by $p[x,t|x(0)] \sim x^{\phi}$.

In the long-time limit we expect $\ell(t)$ to be the only relevant length in the problem. However, the initial separation, $x(0)$, from the absorbing boundary is another length scale, which may become irrelevant only for $\ell(t) \gg x(0)$. To check this assumption we plotted the PDF of unabsorbed particles in terms of the scaled variable $\rho \equiv x/\ell(t)$ for $N=257$ polymers. Figure 4 depicts a sequence of PDFs for $z=2$ ($\alpha=1/2$) at several times. For short times, i.e., when $x(0) \gg \ell(t)$ the maximum of the PDF remains centered close to $x(0)$, and therefore, its center appears near $\rho=x(0)/\ell(t)$, and moves to smaller values of ρ with increasing $\ell(t)$. Indeed this process is clearly seen in Fig. 4 for the three graphs representing the short times, with their maxima moving to the left as $t^{-1/4}$. Graphs corresponding to the two largest times almost coincide representing the final stable shape. Note that this behavior appears in the same range as the apparent power-law behavior of $Q(t)$ in Fig. 2, and above T defined in Eq. (15). To verify the stability of the scaled PDFs it is desirable to study even larger times. Unfortunately, the quality of the graphs deteriorates since the number of surviving diffusers becomes very small.

Figure 5 depicts on a logarithmic scale the PDF of the particle position in terms of the scaled variable $\rho=x/\ell(t)$ for several values of z. Since the evaluation of the probabilities is performed at large times, when only a small fraction of the initial 100 000 samples survives, the statistical fluctuations

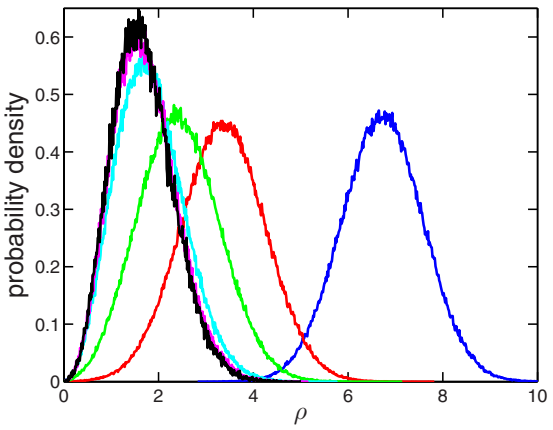

FIG. 4. (Color online) Probability density function of the central monomer $c=129$ in a polymer with $N=257$ monomers in the presence of one absorbing boundary. The monomer is initially located at a distance $8b$ from the absorbing boundary. The horizontal axis is in the scaled variable $\rho=x/\ell(t)$. The graphs correspond to different times (right to left) $t/\tau_s=2,32,128,1024,3500,6000$, and obtained from 100 000 independent runs.

are significant. The figure was obtained by using rather large bins, which poses a problem for a function fast approaching zero. In Fig. 5 about five leftmost points of each graph containing small numbers of events should be disregarded due to statistical uncertainty and more importantly due to the distortion caused by the bin sizes. These effects severely limit the accuracy with which we can determine the exponent ϕ. As a guide to the eyes we have added straight lines with slopes $\phi=1/\alpha$, which seem to provide a fair approximation of the slopes in the range $0.1<\rho<1$. We note that such a form of ϕ describes the behavior near an absorbing wall for Lévy flights [8], as well as for diffusion described by a fractional Laplacian [9] between two absorbing boundaries. Again, as

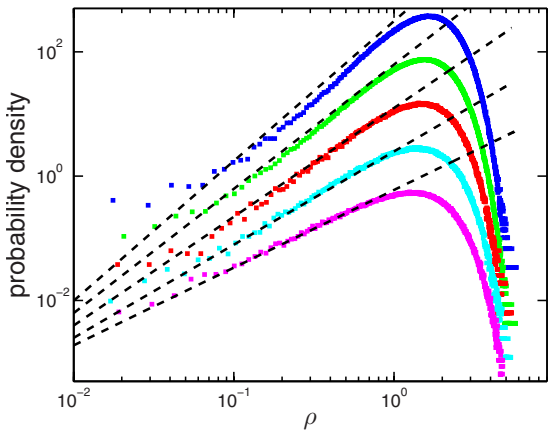

FIG. 5. (Color online) Probability density function of the central particle ($c=129$) in chains of $N=257$ monomers in the presence of one absorbing boundary. The horizontal axis is in the scaled variable $\rho=x/\ell(t)$ (see text). The different curves correspond to $z=1.25$, 1.5, 1.73, 2, and 2.25 (bottom to top). The graphs are shifted vertically for clarity with increasing z values by a factor of 5. The dashed lines have slopes $\phi=1/\alpha$. Each curve was obtained from 100 000 independent runs.

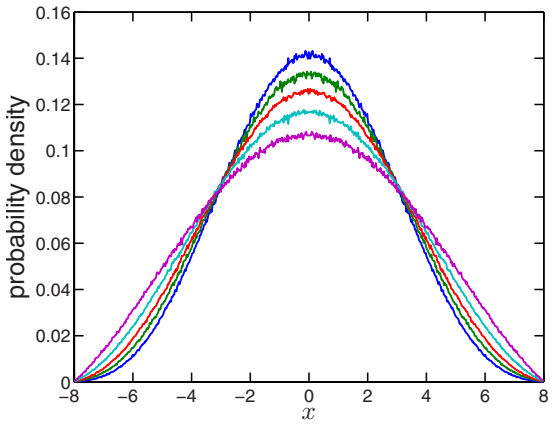

FIG. 6. (Color online) Probability density function of the central particle in a chain with $N=257$ monomers with absorbing boundaries at $X_{b1,2}=\pm 8b$ as a function of position measured from the center of the interval (in units of b) for $z=1.25$, 1.5, 1.75, 2, and 2.25 (broad to narrow). Each graph is the result of 100 000 independent runs.

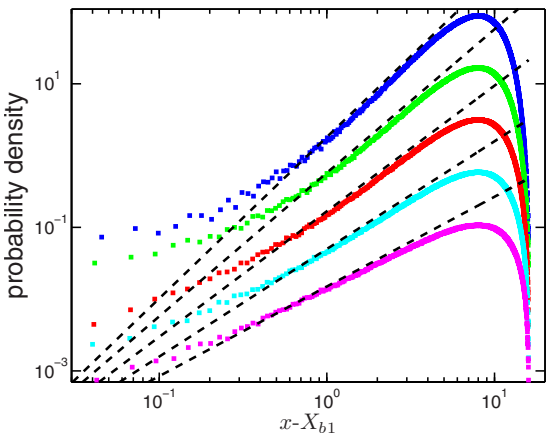

FIG. 7. (Color online) Probability density function of the central monomer in a chain with $N=257$ particles in the presence of absorbing boundaries at $X_{b1}=-8b$ and $X_{b2}=8b$, for $z=1.25$, 1.5, 1.75, 2, and 2.25 (bottom to top). Each curve is the result of 100 000 independent runs. The curves are shifted vertically for clarity, by a factor of 5 at each increasing z. The dashed lines have slopes $\phi=1/\alpha$.

emphasized before, one should beware of possible systematic errors, as the times for which the PDF is measured are not particularly long.

Recently, Zoia *et al.* argued [10] that under rather general assumptions there is a relation between the anomalous diffusion exponent α, the exponent θ governing the tail of the absorption PDF, and the boundary exponent ϕ, given by $\phi=2\theta/\alpha$. Relying on $\theta=1-\alpha/2$ (Ref. [12]), they thus obtain $\phi=2/\alpha-1$ which is larger than the estimates from Fig. 5. On the other hand, using our fits with $\theta\approx\alpha/2$ would yield $\phi\approx 1$, which is smaller than our data indicates.

2. Two absorbing boundaries

In Sec. III A 2 we noted that with two absorbing boundaries the absorption probability eventually decays exponentially. Indeed, the time-dependent PDF for a normal diffuser between two absorbing boundaries is represented by a sum of spatial sinusoidal modes (eigenfunctions of the Laplacian operator) multiplied by functions of time which are pure exponentials. At large times only the lowest harmonic corresponding to the slowest decay, survives. Thus for normal diffusion in the interval between two absorbing boundaries at $X_{b1,2}=\pm 8b$, the spatial probability at long times behaves as $\sim\cos(\pi x/16b)$, again vanishing linearly at the end points. In Ref. [7] it was demonstrated that for $\alpha=1/2$, at times significantly larger than the mean absorption time, the normalized PDF of positions of the surviving tagged monomer has a stable shape different from a cosine.

We performed a detailed study of spatial dependence of the PDF of the surviving anomalous walker between two absorbing boundaries for several values of z. The properly normalized PDF of surviving monomers progresses from a Gaussian with variance growing linearly in time (for $t\ll\tau_s$), to a Gaussian with variance increasing as t^α at intermediate times, before settling down to a stable shape beyond the point of maximum of $Q(t)$ in Fig. 3. Figure 6 depicts these stable shapes for several values of z. Note the nonlinear behavior of the curves near the boundaries. Interestingly the boundary exponent appears to approach $\phi=1$ as $z\to 1$. This is indeed the expected behavior for a normal diffuser, although we note that our diffusers in the limit $z=1$ still reflect the collective behavior of many modes.

To better display the behavior of these stable functions near the boundaries, in Fig. 7 we plot them on a logarithmic scale as a function of a distance from one edge. The results are distorted not only for the reasons mentioned in Sec. III B 1, but also because of the smearing caused by the finite time step of the algorithm (causing a typical step size of each monomer). As in the case of a single absorbing boundary, the dashed lines with slopes $\phi=1/\alpha$ are drawn to guide the eyes. Since the curves have similar shapes and approximately follow a power law near the boundary, we attempted to collapse various curves by raising them to power 2α and normalizing them, but this procedure *did not* result in a good data collapse.

IV. DISCUSSION

A. Comparison with translocation

As we were initially lead to this subject in connection with polymer translocation, it is fitting to conclude by returning to this issue. Translocation, the passage of a polymer through a pore in a membrane, is an important process that has been studied extensively in the last decade [23–30]. Phages, for example, invade bacteria by taking advantage of existing channels in bacterial membranes to translocate their DNA/RNA inside [31]. In theoretical models, it is convenient to study a translocation coordinate s which denotes the number of monomers s on one side of the pore. The dynamics of this coordinate is anomalous: if we assume that the translocation time is of the order of polymer relaxation time τ_0 [27], then the variance of s will increase with time as $t^{\alpha'}$ with $\alpha'=2/(2\nu+1)$ (Rouse dynamics). (For a self-avoiding

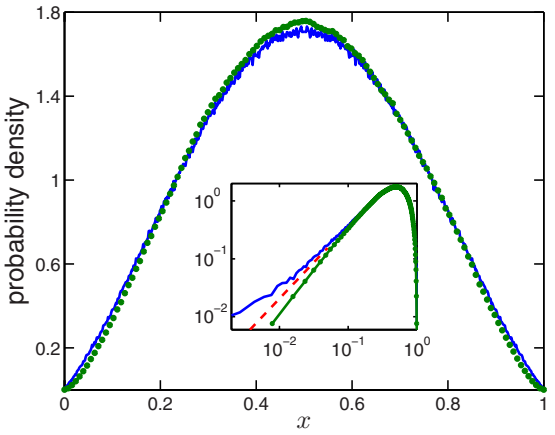

FIG. 8. (Color online) The dots connected by a line depict the normalized PDF of the translocation coordinate, at times significantly exceeding the mean translocation time, for a two-dimensional self-avoiding polymer of length $N=128$ that did not yet translocate (from Ref. [34]). This is compared to the normalized PDF of a central particle (in a chain of $N=257$) performing anomalous diffusion controlled by exponent $z=1.25$ (i.e., $\alpha=0.8$), moving between two absorbing boundaries. For the purpose of comparison the range of the translocation coordinate and the range of monomer positions have been shifted and rescaled to the segment [0,1]. The inset shows the same quantities on the logarithmic scale; the dashed has slope 1.25.

polymer diffusing in 2D, $\nu=3/4$ and $\alpha'=0.8$.) We note that the actual value of the exponent α' also involves factors not explicitly related to the polymer dynamics: (i) that self-avoiding effects expand the equilibrium size of the polymer in the physical space; and (ii) that the relevant variable represents a 1D coordinate in the *internal* space of monomer numbers. While the expression for the actual exponent has been supported numerically in some studies [27,32–35], and disputed in others [36–38], the anomalous nature of dynamics is not in question.

To simplify the process, numerical implementations frequently begin by inserting half of the polymer into the pore [i.e., $s(t=0)\approx N/2$] and allowing the polymer to diffuse until either of its ends ($s=1$ or $s=N$) leaves the pore. This closely resembles the motion of anomalous diffuser in Sec. III B 2 between two absorbing walls, and in a previous work [7] for $\alpha=1/2$. We are now in position to make a more meaningful comparison by choosing a value of z that reproduces the observed exponent for anomalous dynamics of $s(t)$. Specifically, recently Chatelain *et al.* [34] preformed high accuracy simulations of two-dimensional translocation of a self-avoiding polymer. Relevant conclusions from this work are: (a) at short times the distribution of s is almost an exact Gaussian whose variance increases in time with exponent $\alpha'\approx 0.8$. (b) For times larger than the typical translocation time the distribution of translocation time decays exponentially, as in $Q(t)$ in the current work. (c) For times significantly larger than the mean translocation time the PDF of the surviving translocation coordinate qualitatively resembles those in Fig. 6 of Sec. III B 2

In Fig. 8 the results of Ref. [34] are compared with simulations of our model with $z=1.25$ to reproduce the exponent $\alpha=0.8$. For better comparison the allowed interval in both cases is shifted and rescaled to the range between 0 and 1. While the curves are quite similar, they do not coincide. The translocation data are represented by a narrower bell-shaped curve, and close to the boundaries is better described by a power law with exponent $\phi\approx 1.44$ [34], while the curve obtained in our simulations produces a lower exponent of $\phi\approx 1.2$. The differences between the two behaviors is better observed on the logarithmic scale in the inset of Fig. 8. Thus, there are quantitative differences between translocation and anomalous diffusion of a monomer with a similar exponent α.

B. Summary

In this work we concentrated on a group of subdiffusion processes in which a tunable anomalous exponent α is generated through collective behavior of many degrees of freedom. This is achieved by superposition of linear modes in which the relaxation times are scaled by a power law. In the polymer language this corresponds to following a tagged monomer when the friction coefficients of the Rouse modes have a power-law dependence on wavelength. In the absence of absorbing boundaries the model can be solved exactly; starting from a point the PDF of the anomalous walker is a Gaussian whose width grows in time as t^{α}. We were not able to solve the problem in the presence of absorbing boundaries, and resorted to numerical simulations. With a single absorbing point the PDF of absorption decays slowly at long times as $t^{-1-\theta}$. The power-law decay can be justified by noting that the particle can avoid absorption by moving away from the trapping point. A qualitative understanding of the behavior is not yet attained: Estimates based on the fractional Fokker-Planck equation suggest [20] $\theta=\alpha/2$, while an alternative picture from fractional Brownian motion suggests [12] $\theta=1-\alpha/2$. Reference [12] provides numerical support for the latter, while our results are more consistent with the former. The possibility of systematic errors prevents us from making a definite statement on this point, and indicate necessity of further work. When the tagged monomer is confined to an interval bounded by two traps, the survival probability is found to decay exponentially at long times, irrespective of the subdiffusive exponent.

An interesting feature of the process is the vanishing of the PDF on approaching an absorbing boundary (whether single or double). The method of images, which is only valid for regular (Markovian) diffusion, predicts a linear approach to zero, while our simulations indicate a singular form characterized by an exponent ϕ for anomalous walks. While we cannot determine this exponent precisely due to various sampling problems, our results do not appear to support recently proposed exponent relations [10]. The similarities in the shapes of the stable PDFs of surviving walkers in an interval for different values of α, initially raised the hope that they can be collapsed by a simple transformation (e.g., raising them to some power). However, the mismatch between the curves obtained for different exponents α is sufficient to rule out an overarching superuniversality. Furthermore, the discrepancies between translocation of a self-avoiding polymer

and an anomalous diffuser with a similar exponent, suggest that the exponent α is not sufficient to characterize universality. The situation is reminiscent of critical phenomena in which Gaussian (linear) models can be devised to reproduce a particular critical exponent, but which do not capture the full complexity of the nonlinear theory. The absence of definitive agreement between numerics and proposed models is on one hand disappointing, but on the other hand points to the necessity of further work and clarification.

The linear nature of the underlying model raises the hope that exact solutions may be within reach. In the meantime the model does provide a means of generating anomalous walkers with a tunable exponent that incorporate some realistic features of collective dynamics of interacting degrees of freedom. There are certainly puzzles pertaining to the behavior of such anomalous walkers close to an absorbing boundary. To answer these questions simulations need to probe sufficiently short times to remain in the regime of anomalous dynamics, but long enough to ensure convergence to stable forms. Our simulations had a rather limited range of times satisfying the above constraints. While one order of magnitude increase in N could open a broad range of validity of the above conditions, it would significantly slow down the simulations. In addition, working at longer times significantly increases the attrition of the samples, and requires increasing sample size by several orders of magnitude. Currently, such ideal conditions are beyond our numerical abilities, but some improvement over the current results are certainly possible.

ACKNOWLEDGMENTS

We thank S. M. Majumdar, A. Rosso, and A. Zoia for useful advice and discussions. This work was supported by the Israel Science Foundation Grant No. 99/08 (Y.K.) and by the National Science Foundation Grant No. DMR-08-03315 (M.K.). Part of this work was carried out at the Kavli Institute for Theoretical Physics, with support from NSF Grant No. PHY05-51164 (M.K. and Y.K.).

[1] B. B. Mandelbrot and J. W. van Ness, SIAM Rev. **10**, 422 (1968); S. C. Lim and S. V. Muniandy, Phys. Rev. E **66**, 021114 (2002); E. Lutz, *ibid.* **64**, 051106 (2001); A. N. Kolmogorov, C. R. (Dokl.) Acad. Sci. URSS **26**, 6 (1940); K. G. Wang, L. K. Dong, X. F. Wu, F. W. Zhu, and T. Ko, Physica A **203**, 53 (1994); K. G. Wang and M. Tokuyama, *ibid.* **265**, 341 (1999).

[2] R. Metzler and J. Klafter, Phys. Rep. **339**, 1 (2000); J. Phys. A **37**, R161 (2004).

[3] W. Feller, *An Introduction to Probability Theory and Its Applications* (Wiley, New York, 1968).

[4] S. Redner, *A Guide to First-Passage Processes* (Cambridge University Press, Cambridge, England, 2001).

[5] G. H. Weiss, *Aspects and Applications of the Random Walk* (North-Holland, Amsterdam, 1994).

[6] S. B. Yuste and K. Lindenberg, Phys. Rev. E **69**, 033101 (2004); M. Gitterman, *ibid.* **62**, 6065 (2000); **69**, 033102 (2004).

[7] Y. Kantor and M. Kardar, Phys. Rev. E **76**, 061121 (2007).

[8] G. Zumofen and J. Klafter, Phys. Rev. E **51**, 2805 (1995).

[9] A. Zoia, A. Rosso, and M. Kardar, Phys. Rev. E **76**, 021116 (2007).

[10] A. Zoia, A. Rosso, and S. N. Majumdar, Phys. Rev. Lett. **102**, 120602 (2009).

[11] K. Kremer and K. Binder, J. Chem. Phys. **81**, 6381 (1984); G. S. Grest and K. Kremer, Phys. Rev. A **33**, 3628 (1986); I. Carmesin and K. Kremer, Macromolecules **21**, 2819 (1988).

[12] J. Krug, H. Kallabis, S. N. Majumdar, S. J. Cornell, A. J. Bray, and C. Sire, Phys. Rev. E **56**, 2702 (1997).

[13] P.-G. de Gennes, *Scaling Concepts in Polymer Physics* (Cornell University Press, Ithaca, NY, 1979).

[14] M. Doi and S. F. Edwards, *The Theory of Polymer Dynamics* (Clarendon, Oxford, 1986).

[15] P. E. Rouse, J. Chem. Phys. **21**, 1272 (1953).

[16] B. H. Zimm, J. Chem. Phys. **24**, 269 (1956).

[17] M. Kardar, *Statistical Physics of Fields* (Cambridge University Press, Cambridge, England, 2007), Chap. 9.

[18] P. J. Rossky, J. D. Doll, and H. L. Friedman, J. Chem. Phys. **69**, 4628 (1978).

[19] S. Chandrasekhar, Rev. Mod. Phys. **15**, 1 (1943).

[20] V. Balakrishnan, Physica A **132**, 569 (1985); G. Rangarajan and M. Ding, Phys. Rev. E **62**, 120 (2000).

[21] S. Nechaev, G. Oshanin, and A. Blumen, J. Stat. Phys. **98**, 281 (2000).

[22] A. V. Chechkin, R. Metzler, V. Y. Gonchar, J. Klafter, and L. V. Tanatarov, J. Phys. A **36**, L537 (2003).

[23] W. Sung and P. J. Park, Phys. Rev. Lett. **77**, 783 (1996); P. J. Park and W. Sung, J. Chem. Phys. **108**, 3013 (1998).

[24] M. Muthukumar, J. Chem. Phys. **111**, 10371 (1999).

[25] D. K. Lubensky and D. R. Nelson, Biophys. J. **77**, 1824 (1999).

[26] Sh.-Sh. Chern, A. E. Cárdenas, and R. D. Coalson, J. Chem. Phys. **115**, 7772 (2001).

[27] J. Chuang, Y. Kantor, and M. Kardar, Phys. Rev. E **65**, 011802 (2001); Y. Kantor and M. Kardar, *ibid.* **69**, 021806 (2004).

[28] J. J. Kasianowicz, E. Brandin, D. Branton, and D. W. Deamer, Proc. Natl. Acad. Sci. U.S.A. **93**, 13770 (1996).

[29] M. Akeson, D. Branton, J. J. Kasianowicz, E. Brandin, and D. W. Deamer, Biophys. J. **77**, 3227 (1999).

[30] A. Meller, L. Nivon, E. Brandin, J. Golovchenko, and D. Branton, Proc. Natl. Acad. Sci. U.S.A. **97**, 1079 (2000); A. Meller and D. Branton, Electrophoresis **23**, 2583 (2002); A. Meller, L. Nivon, and D. Branton, Phys. Rev. Lett. **86**, 3435 (2001).

[31] B. Dreiseikelmann, Microbiol. Mol. Biol. Rev. **58**, 293 (1994).

[32] K. Luo, T. Ala-Nissila, and S.-Ch. Ying, J. Chem. Phys. **124**, 034714 (2006).

[33] I. Huopaniemi, K. Luo, T. Ala-Nissila, and S.-Ch. Ying, J. Chem. Phys. **125**, 124901 (2006).

[34] C. Chatelain, Y. Kantor, and M. Kardar, Phys. Rev. E **78**, 021129 (2008).

[35] K. Luo, S. T. T. Ollila, I. Huopaniemi, T. Ala-Nissila, P. Po-

morski, M. Karttunen, S.-Ch. Ying, A. Bhattacharya, Phys. Rev. E **78**, 050901(R) (2008).

[36] J. K. Wolterink, G. T. Barkema, and D. Panja, Phys. Rev. Lett. **96**, 208301 (2006); D. Panja, G. T. Barkema, and R. C. Ball, J. Phys. Condens. Matter **19**, 432202 (2007).

[37] J. L. A. Dubbeldam, A. Milchev, V. G. Rostiashvili, and T. A. Vilgis, Phys. Rev. E **76**, 010801(R) (2007).

[38] A. Milchev, K. Binder, and A. Bhattacharya, J. Chem. Phys. **121**, 6042 (2004).